

Direct Stepwise Oxidation of Methane to Methanol over Cu-SiO₂

Selmi Erim Bozbag, Petr Šot, Maarten Nachtegaal, Marco Ranocchiari, Jeroen Anton van Bokhoven, and Carl Mesters

ACS Catal., **Just Accepted Manuscript** • DOI: 10.1021/acscatal.8b01021 • Publication Date (Web): 15 May 2018

Downloaded from <http://pubs.acs.org> on May 15, 2018

Just Accepted

“Just Accepted” manuscripts have been peer-reviewed and accepted for publication. They are posted online prior to technical editing, formatting for publication and author proofing. The American Chemical Society provides “Just Accepted” as a service to the research community to expedite the dissemination of scientific material as soon as possible after acceptance. “Just Accepted” manuscripts appear in full in PDF format accompanied by an HTML abstract. “Just Accepted” manuscripts have been fully peer reviewed, but should not be considered the official version of record. They are citable by the Digital Object Identifier (DOI®). “Just Accepted” is an optional service offered to authors. Therefore, the “Just Accepted” Web site may not include all articles that will be published in the journal. After a manuscript is technically edited and formatted, it will be removed from the “Just Accepted” Web site and published as an ASAP article. Note that technical editing may introduce minor changes to the manuscript text and/or graphics which could affect content, and all legal disclaimers and ethical guidelines that apply to the journal pertain. ACS cannot be held responsible for errors or consequences arising from the use of information contained in these “Just Accepted” manuscripts.



Direct Stepwise Oxidation of Methane to Methanol over Cu-SiO₂

Selmi E. Bozbag^{1,2,†}, Petr Sot^{1,2}, Maarten Nachtegaal¹, Marco Ranocchiari¹, Jeroen A. van Bokhoven^{1,2,}, Carl Mesters^{3,*}*

¹Paul Scherrer Institute, Villigen, CH-5232 Switzerland.

²ETH Zurich, Institute for Chemical and Bioengineering, Wolfgang-Pauli-Strasse 10, CH-8093 Zurich, Switzerland.

³Shell Technology Center Houston, 3333 Highway 6 South, Houston, TX 77083, USA

KEYWORDS: Methane to methanol, silica, copper, activation temperature, XRD, XAS.

ABSTRACT: Cu supported on SiO₂ can be used to directly convert methane to methanol in a step-wise process with no intrinsic need for a zeolite support. Effects of parameters such as the O₂ activation temperature, activation time, CH₄ reaction temperature, CH₄ partial pressure (p_{CH_4}) and Cu wt. % on methanol yield were investigated. Increasing the O₂ activation temperature in the 200-800 °C range significantly improved the methanol yield and when carried out at 800 °C, a methanol yield of 11.5 μmol/g_{catalyst} was obtained after reaction with methane at 200 °C for the sample with 2 wt. % Cu. Yield per mole of Cu increased exponentially from 1.0 to 59.1 mmol with decreased Cu wt. % from 30 to 1, respectively. The increase in the O₂ activation time also

1
2
3 strongly influenced the yield which corresponded to the increase in yield by a factor of >2
4
5 between 1h and 8h. Increasing p_{CH_4} from 0.05 to 1 atm resulted in a 5-fold increase in yield after
6
7 activation at 450 °C however it resulted in at least 20% lower yields after activation at 800 °C
8
9 showing that active sites of different nature were formed at different activation temperatures. The
10
11 increase in yield with ramped O₂ activation temperature correlated with the dehydration of the
12
13 samples as evidenced by X-ray absorption near edge spectroscopy (XANES) and via mass
14
15 spectroscopy (MS) traces of H₂O during the O₂ activation step.
16
17
18
19
20

21 **1. Introduction**

22
23
24 Direct conversion of methane into methanol using molecular oxygen remains one of the
25
26 greatest challenges in catalysis. Although this reaction is thermodynamically possible, it is
27
28 difficult to omit the kinetically controlled over-oxidation of methane since the desired product
29
30 methanol is more reactive. This problem can be addressed by forming a stable complex of the
31
32 reaction intermediate thereby preventing the total oxidation of methane to CO₂ and then
33
34 converting the intermediate to methanol in a step-wise process¹⁻³.
35
36
37
38

39 Over the last decade a number of reports showed the potential of Cu loaded zeolites such as
40
41 ZSM-5⁴, mordenite⁵, small-pore zeolites⁶⁻⁸ and others⁹ for the conversion of methane to
42
43 methanol. The stepwise (sub)stoichiometric process consists of the activation of O₂ on active
44
45 copper-oxo sites¹⁰⁻¹⁴ followed by the reaction of methane in which the oxidized copper sites
46
47 react with methane to form a chemisorbed stable intermediate which allows the production of
48
49 methanol via the subsequent hydration step either at process conditions^{5, 15} or via room
50
51 temperature solvent extraction¹⁶. Processes using oxidants other than O₂¹⁷⁻²¹ and a catalytic
52
53 continuous process were also recently reported²². At ambient pressure, the formation of the
54
55
56
57
58
59
60

1
2
3 active copper-oxo species requires the dehydration of the sample in a high temperature treatment
4 typically $>400\text{ }^{\circ}\text{C}^{23-24}$. At high temperature, the chemisorbed methane intermediate decomposes
5 and therefore the subsequent reaction step is usually carried out at lower temperatures ($<250\text{ }^{\circ}\text{C}$).
6
7
8 The aforementioned stepwise process limits the over-oxidation of the chemisorbed intermediate
9
10 and therefore results in highly selective methanol yields, ranging from 9 to $180\text{ }\mu\text{mol/g}_{\text{catalyst}}$.
11
12 Differences in the yield were associated with the concentration of the active sites and the nature
13
14 of their speciation^{15, 25-26}.
15
16
17
18
19

20 Controllable synthesis of the active copper sites on the zeolite surface is difficult since beside
21 the aforementioned sites a variety of copper species including isolated ions, oligomers, clusters
22 and nanoparticles could form depending on the copper loading, zeolite morphology, Al location
23 within the zeolite and the synthesis method²⁷⁻²⁸. Careful manipulation of the synthesis conditions
24 is necessary for higher yield; Grunder et al. suggested that formation of unselective Cu-oxo
25 clusters can be avoided by limiting the pH during the ion-exchange procedure below the point of
26 zero charge of the surface silanol groups in the zeolite²⁹⁻³⁰. The formation of the active sites in
27 Cu-zeolites has been a subject of many spectroscopic^{23, 27-28, 31-37} and computational studies³⁸⁻⁴².
28
29 A definite agreement about the structure of the active site or sites has not been reached so far.
30
31 For the methane to methanol reaction, the nature and the reactivity of the active site is also
32 highly influenced by the process parameters such as O_2 activation temperature and CH_4 reaction
33 pressure. All of the aforementioned treatments could result in different active site speciation.
34
35 Based on spectroscopic and computational studies, when the process is carried out at ambient
36 pressure with an O_2 activation step $>400\text{ }^{\circ}\text{C}$, mono(μ -oxo)dicopper in Cu-ZSM5⁴³ and Cu-SSZ-
37 13&39⁷, trans- μ -1,2-peroxo dicopper(II) in Cu-SSZ-13&39, tricopper in Cu-HMOR²⁵ and
38
39 tetraneutral clusters in Cu-MOR⁴⁰ were proposed as active sites. Papas et al. showed that the
40
41
42
43
44
45
46
47
48
49
50
51
52
53
54
55
56
57
58
59
60

1
2
3 hydrated $Z[\text{Cu}^{\text{II}}\text{OH}]$ monocopper sites were the precursors to the active sites in Cu-SSZ-13 and
4
5 the activity correlated with the concentration of reducible Cu species⁸. Although absent in
6
7 biological systems, the mono copper core is a thermodynamically favored species in zeolites²³.
8
9 Alayon et al. proposed an additional water-stable active Cu species for Cu-MOR formed upon O_2
10
11 activation at $450\text{ }^\circ\text{C}$ followed by hydration at $200\text{ }^\circ\text{C}$ ⁴⁴. When the step-wise process was carried
12
13 out isothermally at $200\text{ }^\circ\text{C}$ and the subsequent CH_4 reaction step was carried out at high pressure,
14
15 higher methanol yields were obtained and nanoparticles were proposed as the active sites based
16
17 on ultraviolet-visible spectroscopy (UV-Vis) and transmission electron microscopy (TEM)
18
19 data⁴⁵⁻⁴⁶. The complicated formation mechanisms of active copper-oxo sites, which can result in
20
21 a variety of active or inactive Cu species on zeolites, prompted us to investigate supports other
22
23 than zeolites. For the partial oxidation of methane, Cu-SBA15 catalyst showed appreciable
24
25 formaldehyde selectivity at low CH_4 conversions at $625\text{ }^\circ\text{C}$ ⁴⁷. Among other supports, amorphous
26
27 SiO_2 could be an attractive alternative to synthetic zeolites. Cu- SiO_2 using a modified SiO_2 with
28
29 an Al_2O_3 content of 0.6 wt% (Si/Al = 141) did not show appreciable activity for the conversion
30
31 of methane to methanol⁴ most probably due to the absence of active sites which did not form on
32
33 SiO_2 at O_2 activation temperatures below $500\text{ }^\circ\text{C}$. Active Cu-oxo sites might be formed on the
34
35 silica surface at different conditions i.e. at higher O_2 activation temperatures.
36
37
38
39
40
41
42

43 In this study, we show that the direct step-wise conversion of methane to methanol is
44
45 possible on Cu- SiO_2 subsequent to the O_2 activation at higher temperatures ($> 500\text{ }^\circ\text{C}$) without
46
47 the necessity of a zeolite support. The effects of activation temperature, activation duration, CH_4
48
49 partial pressure during reaction and Cu wt. % on the methanol yield were investigated. Cu- SiO_2
50
51 catalysts were characterized using N_2 adsorption, X-ray diffraction (XRD), temperature
52
53 programmed desorption-mass spectroscopy (TPD-MS), UV-Vis, *in-situ* X-ray absorption
54
55
56
57
58
59
60

1
2
3 spectroscopy (XAS) and Scanning transmission electron microscopy (STEM) during or after
4
5 various stages of the catalytic process.
6
7

8 9 **2. Experimental**

10 11 **2.1. Catalyst Preparation and Activity**

12
13
14
15 Cu-SiO₂ with varying Cu loadings (1,2,5,15,30 wt. %) were prepared via pore-volume
16
17 impregnation of a silica support (PQ Silica PD44011) with an ammonium copper carbonate stock
18
19 solution. The ammonium copper carbonate solution was prepared by adding 250 g of (NH₄)₂CO₃
20
21 to 690 g of an ammonia solution (25%). After stirring for 30 min at 30 °C, a clear solution was
22
23 obtained. Subsequently, 300 g of copper hydroxy carbonate was added, in portions of 60 g within
24
25 5 min to the vigorously stirred ammonia carbonate solution. The solution was then diluted to the
26
27 desired metal content and impregnated to the silica support followed by drying at 150 °C and
28
29 calcination at 400 °C. The drying and calcination steps were carried out in air.
30
31
32
33

34
35 The activity tests were carried out in a continuous-flow fixed-bed reactor. The catalyst
36
37 powder (0.7 g) was placed in the middle of a quartz tube reactor which was fitted into a tubular
38
39 furnace. Gas flows were regulated using calibrated mass flow controllers (Bronkhorst). Figure 1
40
41 shows the two different reaction protocols employed. All gas flows were kept at 30 mL/min (1
42
43 atm, 25 °C). The first reaction protocol is hereafter referred to as R1: A stream of O₂ was
44
45 introduced into the reactor and the reactor was heated to the desired activation temperature with
46
47 a ramp of 1 °C/min and remained at this temperature for a desired period. This was followed by
48
49 cooling and removing the excess O₂ with a He stream for 30 min. A CH₄ stream (5% in He) was
50
51 then introduced for 30 min. Finally, the system was cooled down to room temperature under He
52
53 flow for methanol quantification by extraction (described below). The second reaction protocol
54
55
56
57
58
59
60

1
2
3 (hereafter referred to as R2) was similar to that of the first one except methanol was extracted
4 using steam at 200 °C just after the CH₄ reaction step (Step G2 in Figure 1). Steam was supplied
5 using a controlled evaporator mixer (CEM W202A, Bronkhorst) with a rate of 10 g/h where He
6 (30 ml/min) was used as carrier gas. The evaporator temperature was set to 120 °C. All the lines
7 between the evaporator and reactor were heated to 120 °C to avoid condensation. A condenser,
8 cooled down to 15 °C, was connected at the outlet of the reactor where the extract was
9 condensed. Liquid samples containing a mixture of water and methanol were taken from the
10 bottom of the condenser at desired intervals. Once the extraction was completed (as analyzed by
11 gas chromatography (GC), Agilent 6890), a second cycle was initiated with heating from 200 °C
12 in O₂ to the desired activation temperature. Reactor downstream concentrations were monitored
13 using a quadrupole mass spectrometer (Pfeiffer, SEM voltage 1050 V, CH-TRON detector).
14
15
16
17
18
19
20
21
22
23
24
25
26
27
28

29 **2.2. Methanol quantification**

30
31
32 In the first reaction protocol the amount of produced methanol was quantified by extraction
33 with liquid water (Step G1). After the reaction with CH₄ and cooling, the catalyst was transferred
34 into a vial along with a magnetic stirring bar and 2 mL MilliQ water was added. The vial was
35 closed and the mixture was stirred for 2 h. The suspension was filtered through a glass-fiber
36 filter. Afterwards, 10 µl acetonitrile (internal standard, 10% V/V solution in water) was added
37 and the mixture was analyzed on an Agilent 6890 GC equipped with a Restek Rtx®-5 column
38 (30 m, ID = 0.25 mm, film thickness 0.25 µm) and a flame ionization detector. The oven
39 temperature was held at 38 °C for 20 min and subsequently raised to 200 °C at 50 °C/min and
40 held there for 7 min. Solvent extraction was repeated at least twice until no more methanol was
41 obtained. The experimental error in methanol yield was ± 1 µmol/g_{catalyst}. In the second reaction
42
43
44
45
46
47
48
49
50
51
52
53
54
55
56
57
58
59
60

1
2
3 protocol, after the liquid samples were taken from the outlet of the condenser (Step G2),
4
5 acetonitrile was added as internal standard to the sample and the mixture was analyzed by GC.
6
7
8
9
10

11 **2.3.Characterization of the catalysts**

12
13
14
15 Textural properties of the samples were determined by N₂ adsorption using a Micromeritics
16
17 Tristar II 3020 instrument. Approximately 100 mg of each material was transferred into the
18
19 measurement tube, degassed at 50 mTorr at 150 °C overnight and analyzed. The total pore
20
21 volume (V_{total}) was obtained using the uptake amount at $P/P^0 = 0.986$ and micropore volume
22
23 (V_{micro}) was obtained using the t-plot method. The Brunauer, Emmett and Teller (*BET*) surface
24
25 areas of the samples were also measured. XRD measurements were carried out using a Cu K α
26
27 source in a Bruker D8 Advance diffractometer. UV-Vis measurements were carried out in a
28
29 measurement cell which was placed inside a glove bag filled with Ar. After treating the samples
30
31 at various reactive steps described in Fig. 1, Ar was led to flow through the catalyst bed. Then,
32
33 the quartz tubular reactor containing the catalyst bed was quickly removed from the test rig and
34
35 transferred into the glove bag. Catalyst was then transferred into PMMA cuvettes and spectra
36
37 were measured. The UV probe (reflection/backscattering, QR400-7-SR-125F, OD=3.18mm),
38
39 connected by an optical fiber to the spectrometer, was positioned at the center of the PMMA
40
41 cuvette which was fitted on a holder to obtain a good signal to noise ratio. The measurement cell
42
43 was placed in a dark box to minimize stray light. UV-Vis spectra were recorded by a Maya 2000
44
45 Pro (Ocean Optics, Spectra Suite 2000) spectrometer at a scan rate of 200 ms per spectrum from
46
47 35000 cm⁻¹ to 10000 cm⁻¹. A thousand scans were averaged to produce a single spectrum. A
48
49 spectrum of the bare SiO₂ was used as reference. The morphologies of the catalysts were
50
51
52
53
54
55
56
57
58
59
60

1
2
3 characterized by STEM on the aberration-corrected HD-2700CS (Hitachi; cold-field emitter),
4 operated at an acceleration potential of 200 kV. A probe corrector (CEOS) is incorporated in the
5 microscope column between the condenser lens and the probe-forming objective lens providing
6 excellent high-resolution capability (beam diameter ca. 0.1 nm in the selected ultra-high
7 resolution mode). Images (1024 x 1024 pixels) were recorded with a high-angle annular dark
8 field (HAADF) detector with frame times of ca 15 s. These imaging conditions give rise to
9 atomic number (*Z*) contrast, a highly sensitive method to detect even atoms of strongly scattering
10 elements (high *Z*) on light supports. TEM was performed on a F30 microscope (FEI; field
11 emission gun), operated at an acceleration potential of 300 kV. XAS spectra around the Cu K-
12 edge were collected at the SuperXAS beamline, Swiss Light Source (SLS), of the Paul Scherrer
13 Institute in Villigen, Switzerland. The SLS ring is operated in top up mode at 400 mA and 2.4
14 GeV. The polychromatic beam from the 2.9 Tesla superbend source was collimated with a Si-
15 coated collimating mirror at 2.5 mrad. This also served to remove higher harmonics. The X-ray
16 beam was subsequently monochromatized by a channel-cut monochromator using a Si(111)
17 crystal pair. Focusing of the beam to a spot size of 500 x 100 (H x V) micrometer² was achieved
18 using a Rh-coated toroidal mirror. Spectra were measured in transmission mode using 15 cm
19 long ion chambers filled with 20% He/ 80% N₂ mixture resulting in about 8% absorption in both.
20 A Cu foil mounted in front of a third ionization chamber filled with 100% N₂ at 1.5 bar was
21 measured simultaneously and used for absolute energy calibration. Around 15 mg of Cu-SiO₂
22 was fixed between two plugs of quartz wools and placed in a 3 mm diameter, thin-walled quartz
23 capillary reactor. This was affixed to an air blower set-up for controlled heating. The temperature
24 inside the capillary reactor was pre-calibrated against the readout temperature of the blowing hot
25 air with a thermocouple inserted in the reactor until the thermocouple's tip touched the middle of
26
27
28
29
30
31
32
33
34
35
36
37
38
39
40
41
42
43
44
45
46
47
48
49
50
51
52
53
54
55
56
57
58
59
60

the catalyst bed. Subsequently, the thermocouple was removed during the experimental measurements and the air blower was set against the calibrated settings.

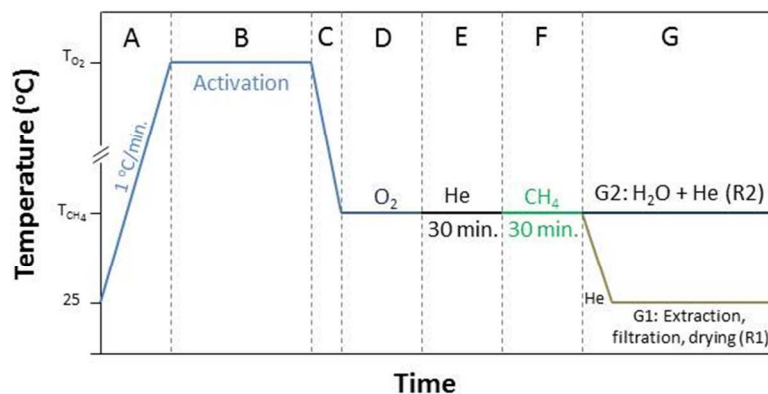


Figure 1. Schematic diagram of the thermal and chemical treatments on Cu-Silica samples during one catalytic cycle. A–D: activation; E: He purge; F: CH₄ reaction; G: hydration and methanol production. (T_{O_2} and T_{CH_4} represent the O₂ activation and CH₄ reaction temperatures, respectively).

3. Results and Discussion

3.1. Catalytic Activity

The samples screened in this study were 1, 2, 5, 15 and 30 wt. % Cu containing Cu-SiO₂ which are hereafter referred to as Cu-SiO₂-1, Cu-SiO₂-2, Cu-SiO₂-5, Cu-SiO₂-15 and Cu-SiO₂-30, respectively. All of the methanol yields reported were obtained using reaction protocol R1 unless otherwise mentioned. The formation of active copper-oxo species in zeolites is significantly influenced by the O₂ activation temperature. Therefore, the effect of the activation temperature on the methanol yield was studied (Fig. 2). For both Cu-SiO₂-2 and Cu-SiO₂-5 very low methanol yields (0.7 $\mu\text{mol}/\text{g}_{\text{catalyst}}$, measured via G1) were obtained up to an activation

1
2
3 temperature of 450 °C followed by exposure to CH₄ (5% CH₄ in He) at 200 °C. Methanol yield
4
5 increased significantly as the O₂ activation temperature increased up to 800 °C reaching 11.5 and
6
7 7.9 μmol/g_{catalyst} for Cu-SiO₂-2 and Cu-SiO₂-5, respectively. The yield obtained from the Cu-
8
9 SiO₂-2 is even higher than that reported for many Cu-zeolite systems^{4,9}. The reusability of the
10
11 Cu-SiO₂-2 in a subsequent catalytic cycle was also tested using reaction protocol R2 and resulted
12
13 in a very similar methanol yield (Fig. 2). When a reaction cycle using Cu-SiO₂-5 with O₂
14
15 activation at 800 °C is followed by a reaction cycle with O₂ activation at 450 °C, the methanol
16
17 yield drops from 7.9 μmol/g_{catalyst} in the 1st cycle to 1.9 μmol/g_{catalyst} in the 2nd cycle showing the
18
19 importance of high temperature activation. Data in Fig. 2 also shows the effect of methane partial
20
21 pressure on the methanol yield. The increase of methane partial pressure from 0.05 to 1 atm
22
23 resulted in an increase of the methanol yield from 0.73 and 0.5 to 4.8 μmol/g_{catalyst} for both
24
25 catalysts after O₂ activation at 450 °C for the Cu-SiO₂-2 and Cu-SiO₂-5, respectively. For the Cu-
26
27 SiO₂-2, the increase of partial pressure increased the yield after O₂ activation at 650 °C but
28
29 decreased the yield after O₂ activation at 800 °C.
30
31
32
33
34
35
36
37
38
39
40
41
42
43
44
45
46
47
48
49
50
51
52
53
54
55
56
57
58
59
60

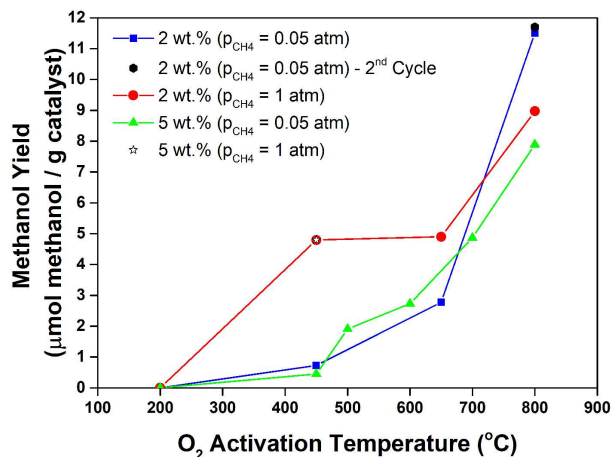


Figure 2. Effect of O₂ activation temperature (for 8 hours) on methanol yield (CH₄ reaction was carried out at 200 °C and the p_{CH₄} denotes the partial pressure of CH₄ during Step F of the catalytic cycle).

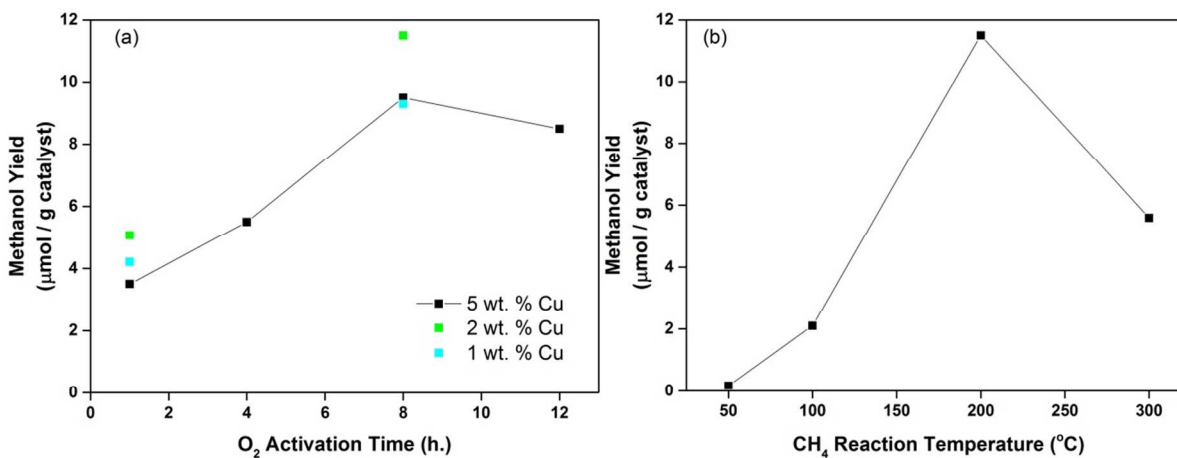


Figure 3. Effect of (a) activation time and (b) CH₄ reaction temperature on the methanol yield. Activation was carried out in O₂ at 800 °C.

Fig. 3a shows the effect of the activation time on the methanol yield when the activation was carried out at 800 °C. Data clearly indicate an increase in methanol yield with activation time up to 8 h where the yield increased from 3.5 to 9.5 μmol/g_{catalyst} for Cu-SiO₂-5. The yield did not

1
2
3 change considerably after an activation time of 12h. Cu-SiO₂-1 and Cu-SiO₂-2 showed a similar
4
5 trend. Thus, with increased O₂ exposure time, the number of reactive sites increased. The
6
7 temperature of the CH₄ reaction step has also an effect on the yield (Fig. 3b). The yield increased
8
9 from 0.2 to 11.5 μmol/g_{catalyst} as the CH₄ reaction temperature was raised from 50 to 200 °C for
10
11 Cu-SiO₂-2. As the CH₄ reaction temperature was further increased to 300 °C, the yield dropped
12
13 to 5.6 μmol/g_{catalyst} due to over-oxidation and the decomposition of the reacted methane
14
15 intermediate. Similar results were also obtained for Cu-chabazite where CH₄ reaction
16
17 temperatures higher than 200 °C resulted in decreased methanol yield and decreased selectivity⁸.
18
19
20
21

22
23 Previous reports on Cu-zeolites showed that the Cu loading is an important parameter that
24
25 affects the methanol yield. Cu loading in zeolites affect the formation of active sites i.e. at lower
26
27 loadings (typically Cu/Al<0.2⁴⁸) monoatomic species exist and as the loading is increased di- or
28
29 tri-copper species or clusters may form. In zeolites active site formation is dictated by the
30
31 location of Al within the framework. Fig. 4 depicts the variation of the methanol yield with Cu
32
33 wt. % in Cu-SiO₂. Different trends in the methanol yield with Cu wt. % were observed for
34
35 different activation temperatures (Fig. 4a). When the O₂ activation was carried out at 800 °C
36
37 followed by CH₄ reaction at 200 °C with a CH₄ partial pressure of 0.05 atm, methanol yield per
38
39 gram catalyst increased with increasing Cu wt. % where the highest value of 11.5 μmol/g_{catalyst}
40
41 was reached with Cu-SiO₂-2. After this point, the yield decreased with increasing Cu wt. %. A
42
43 bare silica sample treated with the same reactive steps of the catalytic cycle as the other catalysts
44
45 did not show any methanol yield (Fig. 4a). When the activation was carried out at 450 °C, the
46
47 yield was considerably smaller for all the samples independent of the metal loading. Cu-SiO₂-1
48
49 did not show any appreciable yield whereas as the metal loading was further increased, the yield
50
51 was increased and a plateau was reached for Cu-SiO₂-2. When the CH₄ partial pressure was 1
52
53
54
55
56
57
58
59
60

1
2
3 atm during the CH₄ reaction step (step F), at least four times higher yields (4.8 μmol/g_{catalyst})
4
5 were obtained as compared to the case of 0.05 atm for both Cu-SiO₂-2 and Cu-SiO₂-5. Lower
6
7 yields were obtained when CH₄ partial pressure was 1 atm after O₂ activation at 800 °C as
8
9 compared to the same case with a CH₄ partial pressure of 0.05 atm. This suggests a difference in
10
11 the nature and the concentration of the active sites for the O₂ activation temperatures of 450 and
12
13 800 °C. Fig. 4b illustrates the variation of the methanol yield per mole of copper in the catalyst.
14
15 After the O₂ activation at 800 °C followed by a CH₄ reaction step at 200 °C (p_{CH₄} = 0.05 atm), the
16
17 methanol yield per mole of Cu increased with decreasing metal loading in the 1-30 wt. % range
18
19 with Cu-SiO₂-1 resulting in a yield of 59.1 mmol/mol Cu. This shows that the concentration of
20
21 the active Cu sites is higher for samples with a lower Cu content. However, the trend upto 2 wt.
22
23 % is different when p_{CH₄} = 1 atm (O₂ activation at 800 °C). Here, the highest yield (per mol of
24
25 Cu) was obtained for the 2 wt. % sample. This again shows that the nature of the active sites
26
27 differs at different CH₄ reaction partial pressures. On the other hand, these different active sites
28
29 may be present for each partial pressure value but with different reaction orders in CH₄
30
31 activation resulting in different methanol yields.
32
33
34
35
36
37
38
39
40
41
42
43
44
45
46
47
48
49
50
51
52
53
54
55
56
57
58
59
60

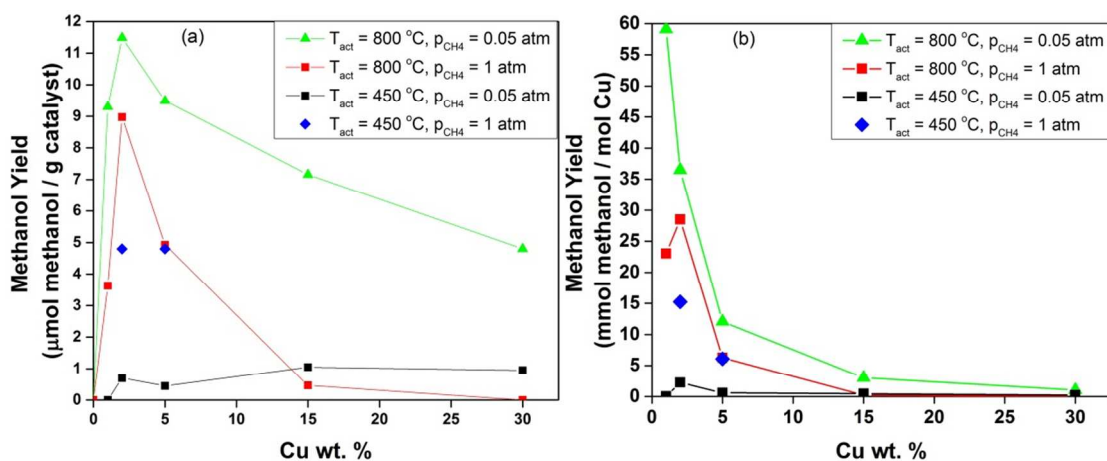


Figure 4. Effect of Cu wt. % on methanol yield. **(a)** micromoles methanol / $\text{g}_{\text{catalyst}}$ **(b)** mmol methanol / mol Cu. p_{CH_4} denotes the partial pressure of CH_4 during Step F of the catalytic cycle.

3.2. Catalyst Characterization

Table 1 shows the textural properties of the samples investigated in this study. The fresh silica sample had a pore volume of $1.65\text{ cm}^3/\text{g}$ with BET surface area of $260\text{ m}^2/\text{g}$ with low concentration of micropores ($0.013\text{ cm}^3/\text{g}$) as compared to the total pore volume. The pore volume and thus the BET surface area decreased from $1.31\text{ cm}^3/\text{g}$ and $276\text{ m}^2/\text{g}$ to $0.70\text{ cm}^3/\text{g}$ and $201\text{ m}^2/\text{g}$ when the Cu wt. % increased from 1 to 30, respectively. At the end of one catalytic cycle, the micropore volume for all samples decreased slightly.

Table 1 Textural properties of the samples

Fresh samples			
Samples	BET surface area (m ² /g)	t-plot Micropore volume (cm ³ /g)	Pore volume (cm ³ /g)
0 (bare silica)	260	0.013	1.65
Cu-SiO ₂ -1	276	0.012	1.31
Cu-SiO ₂ -2	269	0.012	1.34
Cu-SiO ₂ -5	213	0.027	0.98
Cu-SiO ₂ -15	200	0.035	0.77
Cu-SiO ₂ -30	201	0.028	0.70
Post-cycle* samples			
Cu-SiO ₂ -1	240	0.009	1.12
Cu-SiO ₂ -2	229	0.008	1.07
Cu-SiO ₂ -5	200	0.011	1.24
Cu-SiO ₂ -15	204	0.006	0.85
Cu-SiO ₂ -30	184	0.005	0.70

* As depicted in Fig. 1.

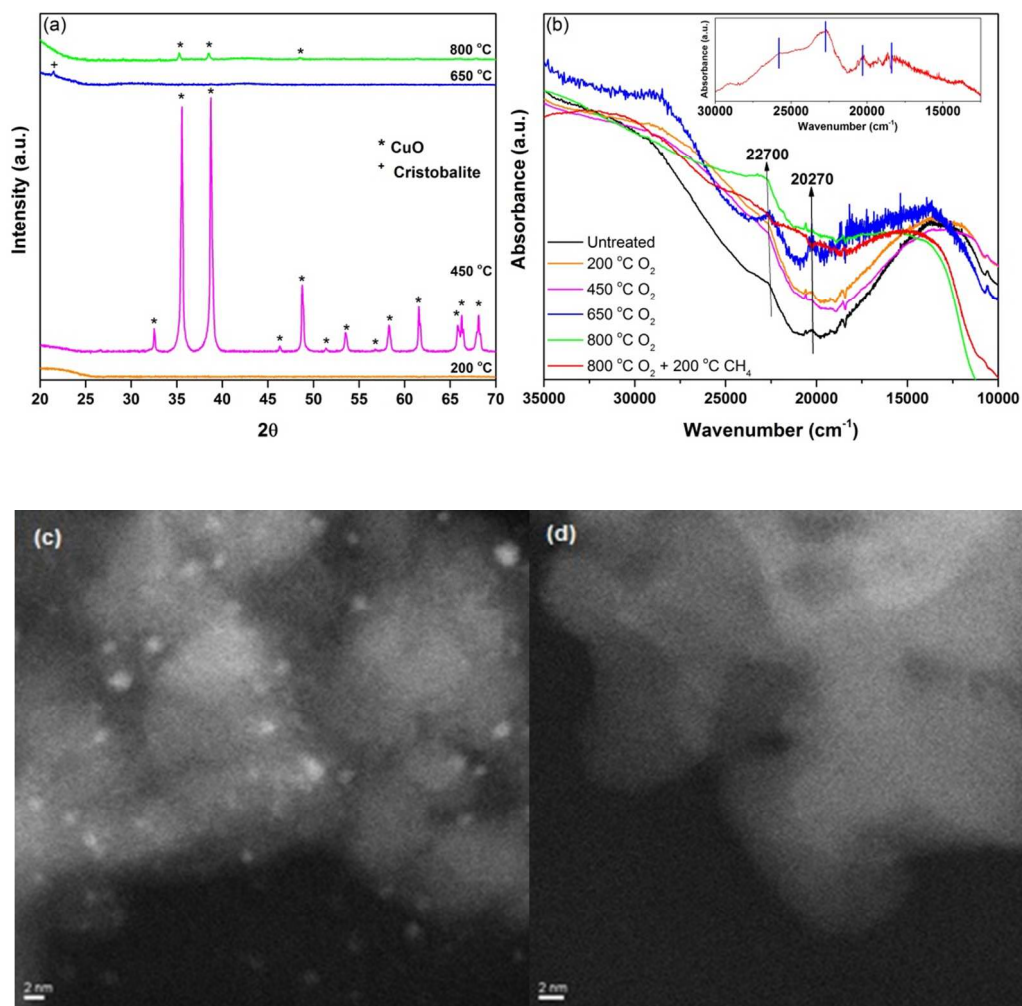


Figure 5. (a) XRD of Cu-SiO₂-2 after calcination at various temperatures in O₂. (b) Room temperature (RT) UV-Vis spectra of Cu-SiO₂-2 after calcination at various temperatures in O₂ and after CH₄ reaction (O₂ activated at 800 °C). Arrows indicate changes in the particular feature with respect to previous temperature increment. Inset shows the difference spectrum between O₂ activated (800 °C) and CH₄ reacted (200 °C) sample. (c) Z-contrast STEM image after O₂ activation at 450 and at (d) 800 °C.

Figure 5 presents the effect of O₂ activation temperature on the structural and spectroscopic features in Cu-SiO₂-2. Fig. 5a shows the XRD patterns after O₂ activation at various temperatures. No crystallinity was observed for either fresh Cu-SiO₂ (not shown) or after the O₂

1
2
3 activation at 200 °C. Monoclinic CuO with sharp peaks were clearly observed after O₂ activation
4
5 at 450 °C with an average diameter of 30 nm as calculated using the Scherrer equation. An
6
7 exemplar STEM image which is shown in Fig. 5c displays well dispersed CuO nanoparticles on
8
9 SiO₂ with average nanoparticle size of 1-2 nm. The small nanoparticles most probably formed
10
11 during the prolonged exposure to the electron beam as illustrated in Fig. 6. Here, one can clearly
12
13 observe the sintering of a CuO nanoparticle indicated with the white arrow until it reaches a size
14
15 of 2.9 nm. This suggests that there is a mixture of bulk CuO crystallites with larger size that were
16
17 absent in the regions analyzed by the STEM and highly dispersed Cu on the surface of SiO₂ after
18
19 the O₂ activation. Surface mixtures of highly dispersed and bulk CuO was also previously
20
21 reported on SiO₂ supported catalysts⁵⁰⁻⁵¹. Further increase in the O₂ activation temperature to 650
22
23 °C resulted in the complete disappearance of the CuO reflections in the XRD pattern. At 650 °C,
24
25 a small peak assigned to cristobalite phase was observed in line with the literature on Cu-SiO₂
26
27 treated at similar temperatures⁵²⁻⁵³. We hypothesize that the disappearance of CuO crystal peaks
28
29 might be due a number of phenomena including the formation of dispersed Cu species, doping of
30
31 Cu into the SiO₂ matrix due to partial crystallization of the support or the formation of
32
33 amorphous islands. At 800 °C, peaks associated with (002) and (111) planes of CuO at 2θ angles
34
35 of 35.4 and 38.7, respectively were observed with a very small intensity indicating that a small
36
37 portion of copper formed CuO crystals. Since the XRD was performed subsequent to the cooling
38
39 down subsequent to the 800 °C O₂ activation, some crystallization might have occurred leading
40
41 to some small CuO reflections. STEM images taken after O₂ activation at 800 °C did not show
42
43 any nanoparticles (Fig 5d). This indicates that CuO nanoparticle concentration is very low and
44
45 the rest of Cu is either in amorphous form or in very small particles that are not detected.
46
47
48
49
50
51
52
53
54
55
56
57
58
59
60

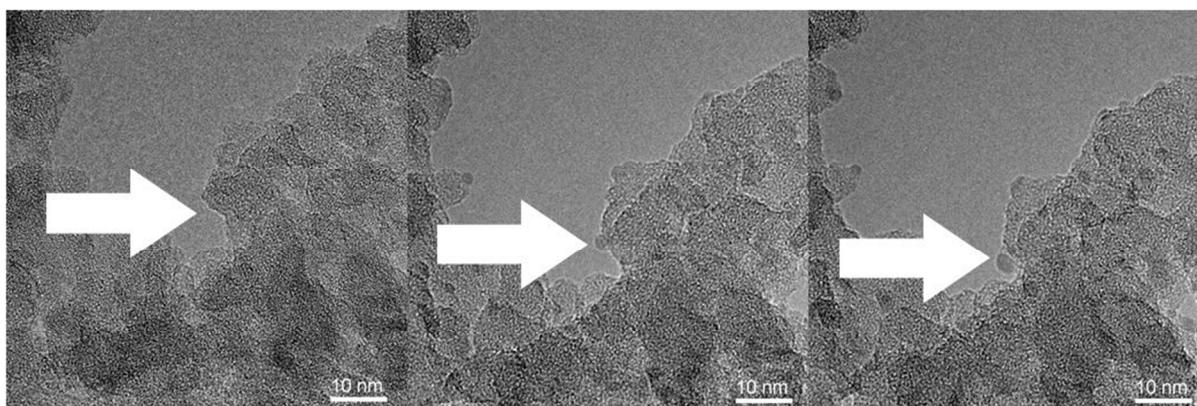
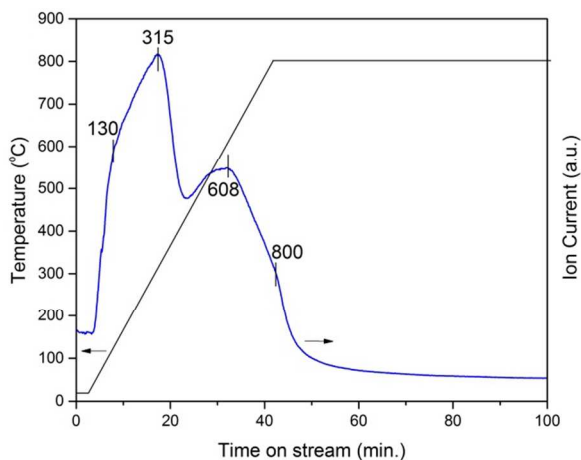


Figure 6. Bright Field TEM image of fresh Cu-SiO₂-15 taken during exposure to the electron beam. The white arrow indicates the growth of a copper oxide nanoparticle on the SiO₂ surface with time.

UV-vis spectroscopy is often used to elucidate the nature of the active copper-oxo sites in Cu-zeolites^{4-5, 32, 54-57}. Fig 5b shows the UV-Vis spectra of the Cu-SiO₂ samples after O₂ activation at various temperatures along with the spectrum taken after the CH₄ reaction at 200 °C (subsequent to O₂ activation at 800 °C). The charge transfer (CT) band at 22700 cm⁻¹ was observed for all samples and its intensity increased with increasing activation temperature. The shape of the band became much more distinct as the O₂ activation temperature was raised above 450 °C. The feature at 22700 cm⁻¹ associated with mono(μ -oxo)dicopper on Cu-ZSM5⁴³ and was also observed in Cu-MOR^{5, 32, 54} was previously suggested as the active site for the direct conversion of methane to methanol. The d-d band at 20000 cm⁻¹ was associated with other active (di-)copper species in zeolites³⁴. The formation of these active (di-)copper species in zeolites was closely associated with the dehydration of the sample therefore we monitored the MS traces of H₂O during the O₂ activation step of Cu-SiO₂-2 (Fig. 7). Here, two broad H₂O desorption peaks could clearly be observed with peak centers at 315 and 608 °C with distinct shoulders at 130 °C, and 800 °C, respectively. The dehydration of Cu-SiO₂ continued with the on-set of an

1
2
3 isothermal dehydration at 800 °C. The dehydration behavior seems to be in line with UV-Vis
4 behavior since the relative intensity of the 22700 cm⁻¹ feature reached its highest value after
5 activation at 800 °C. Dehydration-driven formation of active copper-oxo sites seems to be the
6 case for Cu-SiO₂ as well since the methanol yield increased with increasing O₂ activation
7 temperature (Fig. 2). Formation of the active dicopper is also associated with the Cu/Al ratio^{4,9,}
8⁴⁸ and the proximity of copper ions to the Al ions⁴⁹. Here, we show that at higher O₂ activation
9 temperatures, the 22700 cm⁻¹ feature could manifest on the SiO₂ surface without requiring Al.
10 The feature at 22700 cm⁻¹ observed after O₂ activation at 650 and 800 °C disappeared after
11 subsequent CH₄ reaction at 200 °C (O₂ activated at 800 °C) as shown in Fig 5b and also in the
12 difference spectrum given in the inset of Fig 5b along with other CT features at 25800, 20270
13 and 13380 cm⁻¹ as indicated with blue lines. Gradual disappearance of the 22700 cm⁻¹ feature
14 upon CH₄ reaction^{4-5, 32} or upon NO reaction³⁵ was also observed on Cu-zeolites. Therefore, this
15 feature along with the features observed in the difference spectrum could be ascribed to active
16 site(s) for methane activation on Cu-SiO₂.



17
18
19
20
21
22
23
24
25
26
27
28
29
30
31
32
33
34
35
36
37
38
39
40
41
42
43
44
45
46
47
48
49
50
51
52
53 **Figure 7.** MS traces of H₂O (m/z=18) during the O₂ activation step of Cu-SiO₂-2.
54
55
56
57
58
59
60

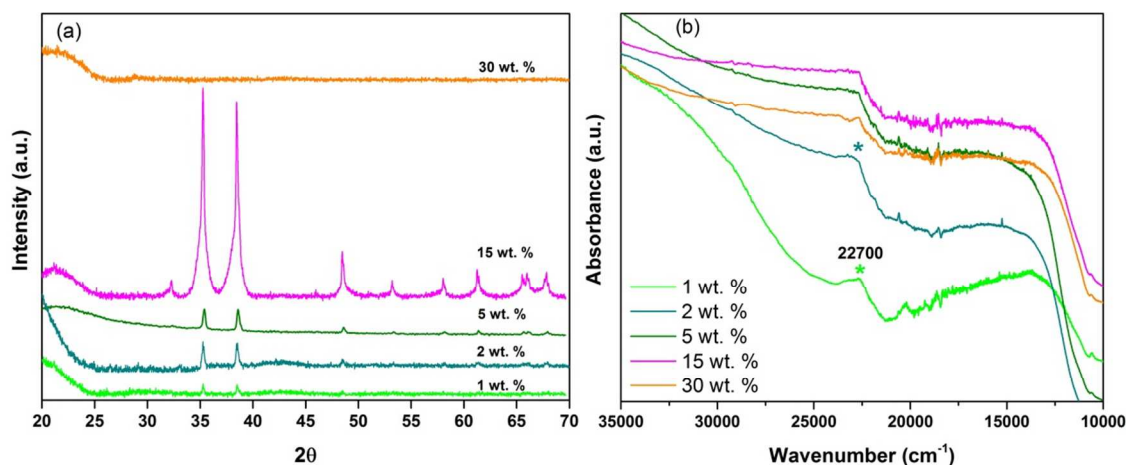


Figure 8. (a) XRD of Cu on silica with various loadings after calcination at 800 °C in O₂. (b) RT UV-Vis spectra of Cu on silica with various loadings after calcination at 800 °C in O₂.

The Cu loading is an important parameter affecting the speciation of the active sites and thus the methanol yield in Cu-zeolites⁴. Therefore, we investigated the effect of metal loading on the structural and spectroscopic features of the Cu-SiO₂ samples after O₂ activation at 800 °C. Samples treated at 800 °C were investigated since they resulted in the highest methanol yields. XRD patterns shown in Fig. 8a indicate the presence of monoclinic CuO in all samples, with the exception of the 30 wt% sample, however the concentration of CuO nanocrystals in the samples varied with metal content. Cu-SiO₂-1 and Cu-SiO₂-2 had a low CuO concentration whereas the concentration of nano-crystals was much higher for Cu-SiO₂-15 which has a bimodal crystal size distribution. The UV-vis spectra illustrated in Fig. 8b again indicates the presence of the 22700 cm⁻¹ feature for all of the samples. However, for samples with loadings higher than 2 wt. % it is difficult to ascribe this feature to a single site due to the bulky shape of the CT region between 35000 and 22000 cm⁻¹. For the Cu-SiO₂-1, a broad CT band at 32200 cm⁻¹ with a shoulder at 29000 cm⁻¹ could also be observed. Similar CT features were ascribed to copper clusters in Cu-zeolites³⁴. Since all the samples had some activity towards the conversion of methane to

methanol, isolated dicopper sites or even CuO clusters with sizes below the detection limit of XRD could be active sites. We performed XRD after all of the relevant subsequent steps of the catalytic cycle for the Cu-SiO₂-2 (Fig. 9). All of the peaks associated with the crystal planes of CuO formed after the O₂ activation at 800 °C, shifted to higher 2θ values upon reaction with CH₄ at 200 °C. This could be associated with the contraction of the crystal lattice⁵⁸ by the chemisorption of reaction intermediates on CuO. Upon subsequent extraction in H₂O (Step G1) which removed the chemisorbed intermediates by the formation of methanol, the XRD showed that the peaks shifted back to their original values obtained after the O₂ activation step however with lower intensity. This indicates that CuO nano-crystals might also be involved in the activation of methane for the production of methanol on Cu-SiO₂

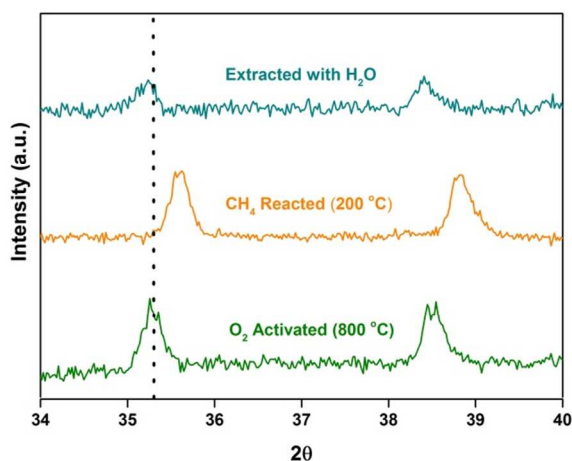


Figure 9. Section of the XRD pattern of Cu-SiO₂-2 after various steps of the catalytic cycle. Dotted line illustrates the 2θ angle of CuO (111) plane.

Fig. 10 compares the XANES and Fourier transformed (FT) extended x-ray absorption fine structure (EXAFS) spectra of Cu-SiO₂-5 (Fig. 10a & c) and Cu-SiO₂-30 (Fig. 10b & d) during progressive heating in O₂ flow. XANES recorded for the Cu-SiO₂-5 sample showed a progressive decrease of the maximum intensity feature at around 9000 eV which indicates a

1
2
3 gradual change in local coordination of Cu with increasing temperature. The distinct shoulder
4
5 observed at around 8986 eV and a pre-edge feature at around 8977 eV are the indications of the
6
7 Cu^{2+} oxidation state. The intensity of this feature slightly increased with increasing temperature
8
9 indicating that the concentration of the Cu^{2+} species increased in agreement with observations of
10
11 Cu species in Cu-zeolites^{15, 23}. The loss of the whiteline intensity can be ascribed to the
12
13 dehydration of the Cu(II) hydroxide species²⁴ as previously demonstrated with the TPD- H_2O
14
15 experiment (Fig. 7). The XANES recorded of the Cu- SiO_2 -30 sample did not show any
16
17 appreciable change in the intensities of neither the whiteline nor the shoulder around 8986 eV
18
19 with increasing temperature from 30 to 800 °C indicating that all Cu was in the form of Cu(II).
20
21
22
23

24
25 The FT EXAFS spectra recorded for the Cu- SiO_2 -5 and Cu- SiO_2 -30 (Fig. 10c&d) during
26
27 progressive heating in O_2 flow show a first coordination shell centered around 1.9 Å (spectra
28
29 were corrected for phase shifts) and a second coordination shell centered around 2.8 Å. For the
30
31 Cu- SiO_2 -5, the increase in the temperature resulted in the change of the shape and the intensity
32
33 of the feature around 1.9 Å most probably due to the loss of coordinated oxygen atoms most
34
35 likely caused by dehydration. FT-EXAFS spectra taken of the Cu- SiO_2 -30 show no significant
36
37 change with increasing temperature similar to the behavior observed during the measurement of
38
39 XANES.
40
41
42
43

44 The EXAFS spectra recorded during the O_2 activation at 800 °C at 5, 60 and 120 min for Cu-
45
46 SiO_2 -5 and Cu- SiO_2 -30 are presented in Fig. 11. No apparent changes were observed in the k^2
47
48 weighted oscillatory functions for both catalysts with changes in O_2 activation time. Given the
49
50 fact that EXAFS is a bulk technique and considering the data in Fig. 3a which shows that the O_2
51
52 activation time is an important parameter for increased methanol yield, indicate that the active
53
54 sites might consist of only a small fraction of the Cu in Cu- SiO_2 .
55
56
57
58
59
60

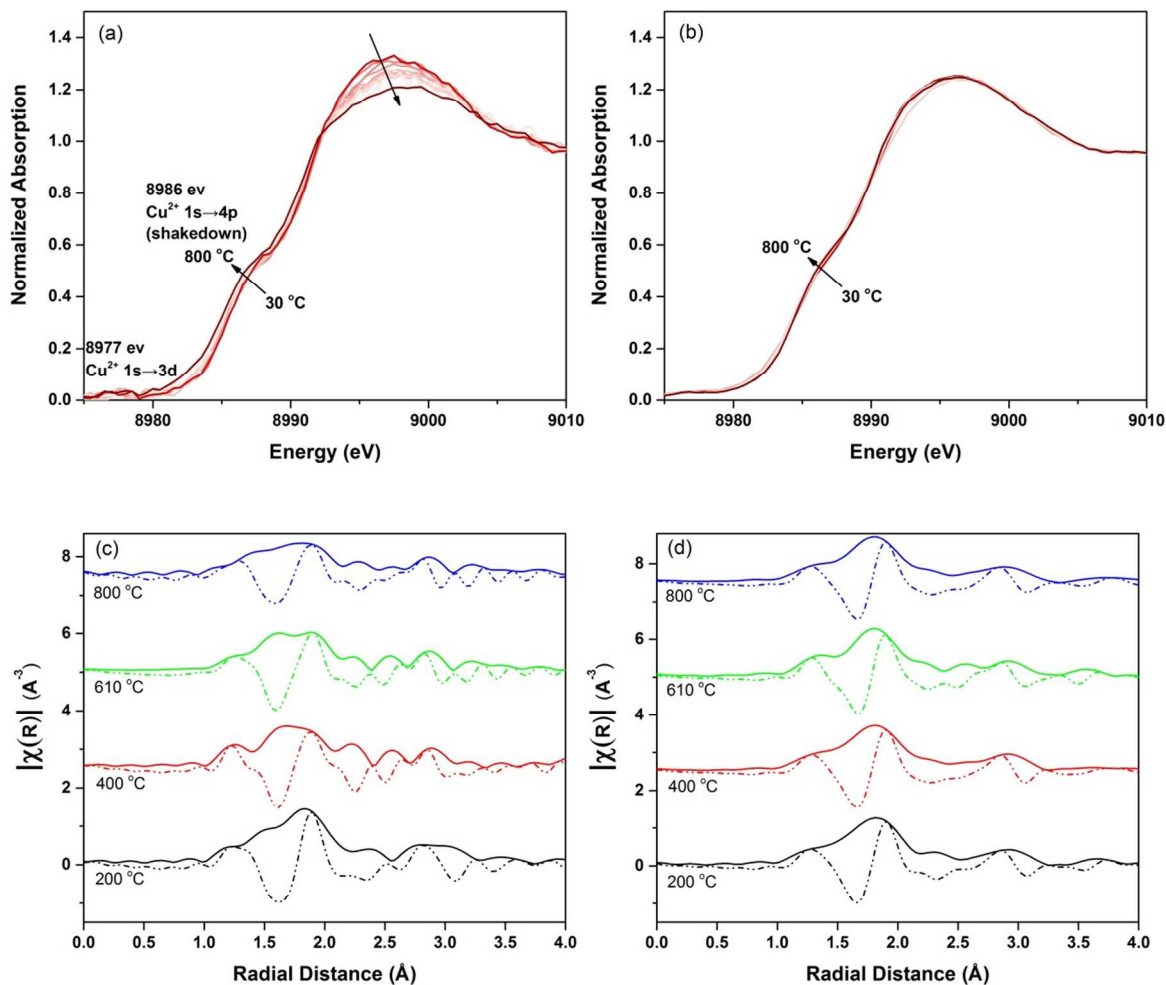


Figure 10. Cu K edge XANES spectra of Cu-SiO₂ samples taken during the O₂ activation period (a) Cu-SiO₂-5, (b) Cu-SiO₂-30. Magnitude of the FT EXAFS spectra and the imaginary part of (c) Cu-SiO₂-5 (d) Cu-SiO₂-30.

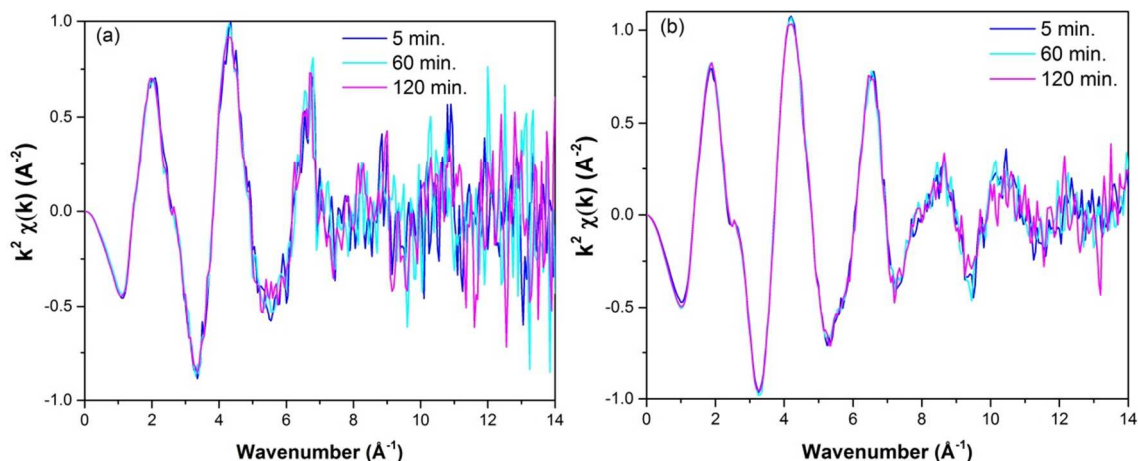


Figure 11. EXAFS spectra of (a) Cu-SiO₂-5, (b) Cu-SiO₂-30 taken during the O₂ activation period at 800 °C.

An important number of articles have appeared for the step-wise direct conversion of methane to methanol since the report of Groothaert et al.⁴ with most of them focusing on the reactivity of transition metal impregnated zeolites. However, Groothaert et al.⁴ had also reported the activity of Cu-SiO₂ with 0.6 wt. % Al₂O₃ and 2 wt. % Cu with a yield of 1 μmol methanol/g_{catalyst}. After activation at 450 °C in O₂ a value slightly higher than our current results (Fig. 2) at the same O₂ activation temperature and Cu wt. % was obtained. This is most probably due to the presence Al in the SiO₂ used⁴ which might have induced the formation of more active sites. The formation of the active Cu-oxo species in zeolites requires the presence of framework Al sites. Addition of Al sites to SiO₂ can create vacancies for the formation of highly dispersed Cu²⁺ species. Reactive copper-oxo species may form on pure silica based supports. For example, Patel et al. suggested that the reduction of NO by CO on copper-oxide supported on mesoporous silica is mostly affected by the presence of dispersed copper species based on H₂-TPR data⁵⁹. An et al.⁶⁰ showed that after calcination at 650 °C, Cu grafted SBA-15 had a mixture of copper-oxo species in the form of dispersed species and clusters, where the increased concentration of dispersed

1
2
3 species correlates with the formaldehyde selectivity. Higher temperature treatment of Cu-SiO₂
4 during O₂ activation might be inducing the formation of dispersed copper-oxo species which are
5 able to activate CH₄ and results in a significantly increased methanol yield. Methanol yields
6 obtained after high temperature O₂ activation on Cu-SiO₂ are higher or similar to those of Cu-
7 MOR⁵ and CuZSM-5^{4,32} with similar Cu metal weight percentages. This shows that the surface
8 concentration of the active sites is similar. On the other hand, high temperature treatment of the
9 Cu-SiO₂ might also have caused changes in the microstructure of the silica support (as indicated
10 by XRD in Fig. 5) as it is very well known that transformations from amorphous silica or from
11 tridymite to cristobalite phase may occur at high temperature in the presence of a catalyst⁶¹⁻⁶⁴.
12 The presence of cristobalite phases in the Mn-Na-W/SiO₂ catalysts was advantageous both for
13 methane conversion and the selectivity for the C₂ species in the oxidative coupling of methane as
14 compared to amorphous silica support⁶³⁻⁶⁴. A similar process may also occur in Cu-SiO₂ catalyst
15 where the crystalline domains could potentially accommodate Cu-oxo species. Using different
16 synthesis routes^{15,25,29} or conducting the CH₄ reaction at high pressure⁴⁵ resulted in much
17 higher methanol yields in Cu-zeolites. This might also be expected for Cu-SiO₂ if different
18 preparation routes and different reactions conditions such as high pressure CH₄ treatment are
19 applied.

4. Conclusion

20
21
22
23
24
25
26
27
28
29
30
31
32
33
34
35
36
37
38
39
40
41
42
43
44
45
46
47
48
49
50
51
52
53
54
55
56
57
58
59
60
Cu-SiO₂ is an effective catalyst for the direct conversion of methane to methanol in a step-
wise manner. The O₂ activation temperature and methane partial pressure affected the methanol
yield significantly. When the activation was carried out at 800 °C, yields similar to that of Cu-
MOR⁵ and Cu-ZSM5⁴ activated at around 400 °C were obtained. The methanol yield was also
affected by the metal content. The yield per mole of copper exponentially increased as the weight

percentage of copper decreased from 30 % to 1 %. Increasing p_{CH_4} from 0.05 to 1 atm resulted in a 5-fold increase in yield after activation at 450 °C, however it resulted in at least 20% lower yields after activation at 800 °C showing that different active sites were formed at different conditions with the possibility of having different reaction orders towards CH₄ activation. UV-Vis suggested that the copper-oxo site associated with the 22700 cm⁻¹ CT band could be one of the active sites. For the Cu-SiO₂-2, XRD indicated the formation of CuO nanoparticles after activation at 450 °C which were absent at 650 °C and appeared again with a much lower concentration at 800 °C. MS signals during the O₂ activation together with the XANES data showed that the formation of the active sites requires the dehydration of the sample. The data presented here showed that formation of active copper species that were previously thought to be formed only on crystalline zeolite supports can be formed on a support material such as SiO₂ if proper conditions are met. Therefore, many other supports might be of use for supporting active Cu species for methane to methanol conversion.

AUTHOR INFORMATION

Corresponding Author

*Corresponding author; e-mail: Carl.Mesters@shell.com; jeroen.vanbokhoven@chem.ethz.ch;

Tel.: + 41 44 632 5542

Present Addresses

†: Koç University, Chemical and Biological Engineering Department, Sarıyer, 34450, Istanbul, Turkey.

Author Contributions

The manuscript was written through contributions of all authors. All authors have given approval to the final version of the manuscript.

ACKNOWLEDGMENT

SEB acknowledges the financial support of Turkish Scientific and Technological Research Council (TÜBİTAK) for the international postdoctoral scholarship (2219). Electron microscopy work was performed at ScopeM (ETH Zurich).

REFERENCES

1. Ahlquist, M.; Nielsen, R. J.; Periana, R. A.; Goddard III, W. A., Product Protection, the Key to Developing High Performance Methane Selective Oxidation Catalysts, *Journal of American Chemical Society* **2009**, 131, 17110-17115.
2. Ravi, M.; Ranocchiari, M.; van Bokhoven, J. A., A Critical Assessment of the Direct Catalytic Oxidation of Methane to Methanol, *Angewandte Chemie International Edition* **2017**.
3. Lange, J. P.; de Jong, K. P.; Ansorge, J.; Tijm, P. J. A., Keys to Methane Conversion Technologies, *Studies in Surface Science and Catalysis* **1997**, 107, 81-86.
4. Groothaert, M. H.; Smeets, P. J.; Sels, B. F.; Jacobs, P. A.; Schoonheydt, R. A., Selective Oxidation of Methane by the Bis(μ -Oxo)Dicopper Core Stabilized on ZSM-5 and Mordenite Zeolites, *Journal of the American Chemical Society* **2005**, 127 (5), 1394-1395.
5. Alayon, E. M.; Nachtegaal, M.; Ranocchiari, M.; van Bokhoven, J. A., Catalytic Conversion of Methane to Methanol over Cu-Mordenite, *Chemical Communications* **2012**, 48 (3), 404-406.
6. Wulfers, M. J.; Teketel, S.; Ipek, B.; Lobo, R. F., Conversion of Methane to Methanol on Copper Containing Small-Pore Zeolites and Zeotypes, *Chemical Communications* **2015**, 51, 4447.
7. Ipek, B.; Wulfers, M. J.; Kim, H.; Göltl, F.; Hermans, I.; Smith, J. P.; Booksh, K. S.; Brown, C. M.; Lobo, R. F., Formation of $[\text{Cu}_2\text{O}_2]^{2+}$ and $[\text{Cu}_2\text{O}]^{2+}$ toward C–H Bond Activation in Cu-SSZ-13 and Cu-SSZ-39, *ACS Catalysis* **2017**, 7 (7), 4291-4303.
8. Pappas, D. K.; Borfecchia, E.; Dyballa, M.; Pankin, I. A.; Lomachenko, K. A.; Martini, A.; Signorile, M.; Teketel, S.; Arstad, B.; Berlier, G.; Lamberti, C.; Bordiga, S.; Olsbye, U.; Lillerud, K. P.; Svelle, S.; Beato, P., Methane to Methanol: Structure–Activity Relationships for Cu-CHA, *Journal of the American Chemical Society* **2017**, 139 (42), 14961-14975.
9. Park, M. B.; Ahn, S. H.; Ranocchiari, M.; van Bokhoven, J. A., Comparative Study of Diverse Cu-Zeolites for Conversion of Methane-to-Methanol, *ChemCatChem* **2017**.

10. Labinger, J. A., Selective Alkane Oxidation: Hot and Cold Approaches to a Hot Problem, *Journal of Molecular Catalysis A: Chemical* **2004**, 220 (1), 27-35.
11. Chen, P. P. Y.; Yang, R. B. G.; Lee, J. C. M.; Chan, S. I., Facile O-Atom Insertion into C-C and C-H Bonds by a Trinuclear Copper Complex Designed to Harness a Singlet Oxene, *Proc. Natl. Acad. Sci. U. S. A.* **2007**, 104 (37), 14570-14575.
12. Que, L.; Tolman, W. B., Biologically Inspired Oxidation Catalysis, *Nature* **2008**, 455 (7211), 333-340.
13. Balasubramanian, R.; Smith, S. M.; Rawat, S.; Yatsunyk, L. A.; Stemmler, T. L.; Rosenzweig, A. C., Oxidation of Methane by a Biological Dicopper Centre, *Nature* **2010**, 465 (7294), 115-U131.
14. Haack, P.; Limberg, C., Molecular CuII-O-CuII Complexes: Still Waters Run Deep, *Angewandte Chemie-International Edition* **2014**, 53 (17), 4282-4293.
15. Bozbag, S. E.; Alayon, E. M. C.; Pechacek, J.; Nachtegaal, M.; Ranocchiari, M.; van Bokhoven, J. A., Methane to Methanol over Copper Mordenite: Yield Improvement through Multiple Cycles and Different Synthesis Techniques, *Catalysis Science & Technology* **2016**, 6 (13), 5011-5022.
16. Beznis, N. V.; Weckhuysen, B. M.; Bitter, J. H., Cu-ZSM-5 Zeolites for the Formation of Methanol from Methane and Oxygen: Probing the Active Sites and Spectator Species, *Catal. Lett.* **2010**, 138 (1-2), 14-22.
17. Kim, Y.; Kim, T. Y.; Lee, H.; Yi, J., Distinct Activation of Cu-MOR for Direct Oxidation of Methane to Methanol, *Chemical Communications* **2017**, 53 (29), 4116-4119.
18. Sheppard, T.; Hamill, C. D.; Goguet, A.; Rooney, D. W.; Thompson, J. M., A Low Temperature, Isothermal Gas-Phase System for Conversion of Methane to Methanol over Cu-ZSM-5, *Chemical Communications* **2014**, 50, 11053-11055.
19. Sushkevich, V. L.; Palagin, D.; Ranocchiari, M.; van Bokhoven, J. A., Selective Anaerobic Oxidation of Methane Enables Direct Synthesis of Methanol, *Science* **2017**, 356 (6337), 523-527.
20. Hutchings, G. J., Methane Activation by Selective Oxidation, *Top. Catal.* **2016**, 59 (8-9), 658-662.
21. Tsai, M. L.; Hadt, R. G.; Vanelderen, P.; Sels, B. F.; Schoonheydt, R. A.; Solomon, E. I., Cu₂O (2+) Active Site Formation in Cu-ZSM-5: Geometric and Electronic Structure Requirements for N₂O Activation, *Journal of the American Chemical Society* **2014**, 136 (9), 3522-3529.
22. Narsimhan, K.; Iyoki, K.; Dinh, K.; Roman-Leshkov, Y., Catalytic Oxidation of Methane into Methanol over Copper-Exchanged Zeolites with Oxygen at Low Temperature, *ACS Central Science* **2016**, 2 (6), 424-429.
23. Alayon, E. M. C.; Nachtegaal, M.; Bodi, A.; Ranocchiari, M.; van Bokhoven, J. A., Bis(μ -Oxo) Versus Mono(μ -Oxo)Dicopper Cores in a Zeolite for Converting Methane to Methanol: An in Situ Xas and Dft Investigation, *Physical Chemistry Chemical Physics* **2015**, 17 (12), 7681-7693.
24. Borfecchia, E.; Lomachenko, K. A.; Giordanino, F.; Falsig, H.; Beato, P.; Soldatov, A. V.; Bordiga, S.; Lamberti, C., Revisiting the Nature of Cu Sites in the Activated Cu-SSZ-13 Catalyst for Scr Reaction, *Chemical Science* **2015**, 6 (1), 548-563.
25. Grundner, S.; Markovits, M. A. C.; Li, G.; Tromp, M.; Pidko, E. A.; Hensen, E. J. M.; Jentys, A.; Sanchez-Sanchez, M.; Lercher, J. A., Single-Site Trinuclear Copper Oxygen Clusters

1
2
3 in Mordenite for Selective Conversion of Methane to Methanol, *Nature Communications* **2015**,
4 6.

5 26. Alayon, E. M. C.; Nachtegaal, M.; Kleymenov, E.; van Bokhoven, J. A., Determination
6 of the Electronic and Geometric Structure of Cu Sites During Methane Conversion over Cu-Mor
7 with X-Ray Absorption Spectroscopy, *Microporous and Mesoporous Materials* **2013**, 166 (0),
8 131-136.

9 27. LoJacono, M.; Fierro, G.; Dragone, R.; Feng, X. B.; dltri, J.; Hall, W. K., Zeolite
10 Chemistry of Cuzsm-5 Revisited, *J. Phys. Chem. B* **1997**, 101 (11), 1979-1984.

11 28. Kuroda, Y.; Konno, S.; Yoshikawa, Y.; Maeda, H.; Kubozono, Y.; Hamano, H.;
12 Kumashiro, R.; Nagao, M., Stabilization of Copper Metal Clusters in Mordenite Micropores -
13 Water Treatment of Evacuated Copper Ion-Exchanged Mordenite at 300 K, *J. Chem. Soc.-*
14 *Faraday Trans.* **1997**, 93 (11), 2125-2130.

15 29. Grundner, S.; Luo, W.; Sanchez-Sanchez, M.; Lercher, J. A., Synthesis of Single-Site
16 Copper Catalysts for Methane Partial Oxidation, *Chemical Communications* **2016**, 52 (12), 2553-
17 2556.

18 30. Sheppard, T.; Daly, H.; Goguet, A.; Thompson, J. M., Improved Efficiency for Partial
19 Oxidation of Methane by Controlled Copper Deposition on Surface-Modified ZSM-5,
20 *Chemcatchem* **2016**, 8 (3), 562-570.

21 31. Llabrés i Xamena, F. X.; Fiscaro, P.; Berlier, G.; Zecchina, A.; Palomino, G. T.;
22 Prestipino, C.; Bordiga, S.; Giamello, E.; Lamberti, C., Thermal Reduction of Cu²⁺-Mordenite
23 and Re-Oxidation Upon Interaction with H₂O, O₂, and NO, *The Journal of Physical Chemistry B*
24 **2003**, 107 (29), 7036-7044.

25 32. Smeets, P. J.; Groothaert, M. H.; Schoonheydt, R. A., Cu Based Zeolites: A Uv-Vis
26 Study of the Active Site in the Selective Methane Oxidation at Low Temperatures, *Catal. Today*
27 **2005**, 110 (3-4), 303-309.

28 33. Palomino, G. T.; Fiscaro, P.; Bordiga, S.; Zecchina, A.; Giamello, E.; Lamberti, C.,
29 Oxidation States of Copper Ions in Zsm-5 Zeolites. A Multitechnique Investigation, *The Journal*
30 *of Physical Chemistry B* **2000**, 104 (17), 4064-4073.

31 34. Giordanino, F.; Vennestrom, P. N. R.; Lundegaard, L. F.; Stappen, F. N.; Mossin, S.;
32 Beato, P.; Bordiga, S.; Lamberti, C., Characterization of Cu-Exchanged SSZ-13: A Comparative
33 Ftir, Uv-Vis, and Epr Study with Cu-ZSM-5 and Cu-Beta with Similar Si/Al and Cu/Al Ratios,
34 *Dalton Transactions* **2013**, 42 (35), 12741-12761.

35 35. Groothaert, M. H.; van Bokhoven, J. A.; Battiston, A. A.; Weckhuysen, B. M.;
36 Schoonheydt, R. A., Bis(μ-Oxo)Dicopper in Cu-ZSM-5 and Its Role in the Decomposition of
37 No: A Combined in Situ Xafs, UV-Vis-near-IR, and Kinetic Study, *Journal of the American*
38 *Chemical Society* **2003**, 125 (25), 7629-7640.

39 36. Bordiga, S.; Groppo, E.; Agostini, G.; van Bokhoven, J. A.; Lamberti, C., Reactivity of
40 Surface Species in Heterogeneous Catalysts Probed by In Situ X-ray Absorption Techniques,
41 *Chemical Reviews* **2013**, 113 (3), 1736-1850.

42 37. van Bokhoven, J. A.; Lamberti, C., *X-Ray Absorption and X-ray Emission Spectroscopy:*
43 *Theory and Applications*. John Wiley & Sons: Chichester (UK), 2016.

44 38. Zhao, Z. J.; Kulkarni, A.; Vilella, L.; Norskov, J. K.; Studt, F., Theoretical Insights into
45 the Selective Oxidation of Methane to Methanol in Copper-Exchanged Mordenite, *Acs Catalysis*
46 **2016**, 6 (6), 3760-3766.

- 1
2
3 39. Kulkarni, A. R.; Zhao, Z. J.; Siahrostami, S.; Norskov, J. K.; Studt, F., Monocopper
4 Active Site for Partial Methane Oxidation in Cu-Exchanged 8mr Zeolites, *Acs Catalysis* **2016**, 6
5 (10), 6531-6536.
6
7 40. Palagin, D.; Knorpp, A. J.; Pinar, A. B.; Ranocchiari, M.; van Bokhoven, J. A., Assessing
8 the Relative Stability of Copper Oxide Clusters as Active Sites of a Cumor Zeolite for Methane
9 to Methanol Conversion: Size Matters?, *Nanoscale* **2017**, 9 (3), 1144-1153.
10
11 41. Yumura, T.; Hirose, Y.; Wakasugi, T.; Kuroda, Y.; Kobayashi, H., Roles of Water
12 Molecules in Modulating the Reactivity of Dioxygen-Bound Cu-Zsm-5 toward Methane: A
13 Theoretical Prediction, *Acs Catalysis* **2016**, 6 (4), 2487-2495.
14
15 42. Mahyuddin, M. H.; Staykov, A.; Shiota, Y.; Yoshizawa, K., Direct Conversion of
16 Methane to Methanol by Metal-Exchanged Zsm-5 Zeolite (Metal = Fe, Co, Ni, Cu), *Acs*
17 *Catalysis* **2016**, 6 (12), 8321-8331.
18
19 43. Woertink, J. S.; Smeets, P. J.; Groothaert, M. H.; Vance, M. A.; Sels, B. F.; Schoonheydt,
20 R. A.; Solomon, E. I., A Cu₂O (2+) Core in Cu-ZSM-5, the Active Site in the Oxidation of
21 Methane to Methanol, *Proc. Natl. Acad. Sci. U. S. A.* **2009**, 106 (45), 18908-18913.
22
23 44. Alayon, E. M. C.; Nachtegaal, M.; Bodi, A.; van Bokhoven, J. A., Reaction Conditions of
24 Methane-to-Methanol Conversion Affect the Structure of Active Copper Sites, *ACS Catalysis*
25 **2014**, 4 (1), 16-22.
26
27 45. Tomkins, P.; Mansouri, A.; Bozbag, S. E.; Krumeich, F.; Park, M. B.; Alayon, E. M. C.;
28 Ranocchiari, M.; van Bokhoven, J. A., Isothermal Cyclic Conversion of Methane into Methanol
29 over Copper-Exchanged Zeolite at Low Temperature, *Angewandte Chemie-International Edition*
30 **2016**, 55 (18), 5467-5471.
31
32 46. Tomkins, P.; Ranocchiari, M.; van Bokhoven, J. A., Direct Conversion of Methane to
33 Methanol under Mild Conditions over Cu-Zeolites and Beyond, *Accounts of Chemical Research*
34 **2017**, 50 (2), 418-425.
35
36 47. Li, Y.; An, D.; Zhang, Q.; Wang, Y., Copper-Catalyzed Selective Oxidation of Methane
37 by Oxygen: Studies on Catalytic Behavior and Functioning Mechanism of Cuox/Sba-15, *J. Phys.*
38 *Chem. C* **2008**, 112, 13700-13708.
39
40 48. Vanelderen, P.; Hadt, R. G.; Smeets, P. J.; Solomon, E. I.; Schoonheydt, R. A.; Sels, B.
41 F., Cu-Zsm-5: A Biomimetic Inorganic Model for Methane Oxidation, *J. Catal.* **2011**, 284 (2),
42 157-164.
43
44 49. Markovits, M. A. C.; Jentys, A.; Tromp, M.; Sanchez-Sanchez, M.; Lercher, J. A., Effect
45 of Location and Distribution of Al Sites in Zsm-5 on the Formation of Cu-oxo Clusters Active
46 for Direct Conversion of Methane to Methanol, *Top. Catal.* **2016**, 59 (17-18), 1554-1563.
47
48 50. Huang, Z.; Cui, F.; Kang, H.; Chen, J.; Zhang, X.; Xia, C., Highly Dispersed Silica-
49 Supported Copper Nanoparticles Prepared by Precipitation-Gel Method: A Simple but Efficient
50 and Stable Catalyst for Glycerol Hydrogenolysis, *Chem. Mater.* **2008**, 20, 5090-5099.
51
52 51. Zhang, R.; Sun, Y.-h.; Peng, S.-y., Dehydrogenation of Methanol to Methyl Formate over
53 CuO-SiO₂ Gel Catalyst, *Reaction Kinetics and Catalysis Letters* **1999**, 67, 95-102.
54
55 52. de Sousa, E. M. B.; de Magalhaes, W. F.; Mohallem, N. D. S., Characterization of Silica
56 Nanocomposites Obtained by Sol-Gel Process Using Positron Annihilation Spectroscopy,
57 *Journal of Physics and Chemistry of Solids* **1999**, 60 211-221.
58
59 53. Sivasubramanian, G.; Shanmugam, C.; Parameswaran, V. R., Copper(II) Immobilized on
60 Silica Extracted from Foxtail Millet Husk: A Heterogeneous Catalyst for the Oxidation of
Tertiary Amines under Ambient Conditions, *Journal of Porous Materials* **2013**, 20, 417-430.

- 1
2
3 54. Vanelderen, P.; Vancauwenbergh, J.; Tsai, M.-L.; Hadt, R. G.; Solomon, E. I.;
4 Schoonheydt, R. A.; Sels, B. F., Spectroscopy and Redox Chemistry of Copper in Mordenite,
5 *Chemphyschem* **2014**, 15 (1), 91-99.
6
7 55. Le, H. V.; Parishan, S.; Saaltchik, A.; Gobel, C.; Schlesiger, C.; Malzer, W.; Trunschke,
8 A.; Schomacker, R.; Thomas, A., Solid-State Ion-Exchanged Cu/Mordenite Catalysts for the
9 Direct Conversion of Methane to Methanol, *Acs Catalysis* **2017**, 7 (2), 1403-1412.
10
11 56. Narsimhan, K.; Michaelis, V. K.; Mathies, G.; Gunther, W. R.; Griffin, R. G.; Roman-
12 Leshkov, Y., Methane to Acetic Acid over Cu-Exchanged Zeolites: Mechanistic Insights from a
13 Site-Specific Carbonylation Reaction, *Journal of the American Chemical Society* **2015**, 137 (5),
14 1825-1832.
15
16 57. Verma, A. A.; Bates, S. A.; Anggara, T.; Paolucci, C.; Parekh, A. A.; Kamasamudram,
17 K.; Yezerets, A.; Miller, J. T.; Delgass, W. N.; Schneider, W. F.; Ribeiro, F. H., No Oxidation: A
18 Probe Reaction on Cu-Ssz-13, *J. Catal.* **2014**, 312, 179-190.
19
20 58. Bozbag, S. E.; Unal, U.; Kurykin, M. A.; Ayala, C. J.; Aindow, M.; Erkey, C.,
21 Thermodynamic Control of Metal Loading and Composition of Carbon Aerogel Supported Pt-
22 Cu Alloy Nanoparticles by Supercritical Deposition, *Journal Physical Chemistry C* **2013**, 117,
23 6777.
24
25 59. Patel, A.; Shukla, P.; Rufford, T.; Wang, S.; Chen, J.; Rudolph, V.; Zhu, Z., Catalytic
26 Reduction of NO by CO over Copper-Oxide Supported Mesoporous Silica, *Applied Catalysis A:*
27 *General* **2011**, 55-65, 409-410.
28
29 60. An, D.; Zhang, Q.; Wang, Y., Copper Grafted on SBA-15 as Efficient Catalyst for the
30 Selective Oxidation of Methane by Oxygen, *Catal. Today* **2010**, 157 143-148
31
32 61. Roy, D. M.; Roy, R. Tridymite-cristobalite relations and stable solid solutions. *The*
33 *American Mineralogist* **1964**, 49, 952-962.
34
35 62. Arahori, T.; Suzuki, T. Transformation of tridymite to cristobalite below 1470°C in silica
36 refractories. *Journal of Materials Science* **1987**, 22, 2248-2252.
37
38 63. Ji, S.; Xiao, T.; Li, S.; Chou, L.; Zhang, B.; Xu, C.; Hou, R.; York, A. P. E.; Green, M. L.
39 H. Surface WO₄ tetrahedron: the essence of the oxidative coupling of methane over M-W-
40 Mn/SiO₂ catalysts. *J. Catal.* **2003**, 220 47-56.
41
42 64. Palermo, A.; Vazquez, J. P. H.; Lee, A. F.; Tikhov, M. S.; Lambert, R. M. Critical
43 Influence of the Amorphous Silica-to-Cristobalite Phase Transition on the Performance of
44 Mn/Na₂WO₄/SiO₂ Catalysts for the Oxidative Coupling of Methane. *J. Catal.* **1998**, 177, 259-
45 266.
46
47
48
49
50
51
52
53
54
55
56
57
58
59
60

Table of contents image

